Article

Deuterium NMR of Raft Model Membranes Reveals Domain-Specific Order Profiles and Compositional Distribution

Tomokazu Yasuda,[1,2] Hiroshi Tsuchikawa,[1] Michio Murata,[1,2] and Nobuaki Matsumori[1,*]
[1]Department of Chemistry, Graduate School of Science, Osaka University, Toyonaka, Osaka, Japan; and [2]Japan Science and Technology Agency, ERATO, Lipid Active Structure Project, Toyonaka, Osaka, Japan

ABSTRACT In this report, we applied site-specifically deuterated *N*-stearoylsphingomyelins (SSMs) to raft-exhibiting ternary mixtures containing SSM, 1,2-dioleoyl-*sn*-glycero-3-phosphocholine (DOPC), and cholesterol (Chol) and successfully acquired deuterium quadrupole coupling profiles of SSM from liquid-ordered (L_o) and liquid-disordered (L_d) domains. To our knowledge, this is the first report that shows detailed lipid chain dynamics separately and simultaneously obtained from coexisting L_o and L_d domains. We also found that the quadrupole profile of the L_o phase in the ternary system was almost identical to that in the SSM-Chol binary mixture, suggesting that the order profile of the binary system is essentially applicable to more complicated membrane systems in terms of the acyl chain order. We also demonstrated that ^{2}H NMR spectroscopy, in combination with organic synthesis of deuterated components, could be used to reveal the accurate mole fractions of each component distributed in the L_o and L_d domains. As compared with the reported tie-line analysis of phase diagrams, the merit of our ^{2}H NMR analysis is that the domain-specific compositional fractions are directly attainable without experimental complexity and ambiguity. The accurate compositional distributions as well as lipid order profiles in ternary mixtures are relevant to understanding the molecular mechanism of lipid raft formation.

INTRODUCTION

Since the lipid raft hypothesis was postulated in the late 1990s (1), lipid rafts have been shown to play significant roles in cellular processes, including signal transduction, protein sorting, and microbial infection (2–6). The physical properties of raft domains are comparable with those of a liquid-ordered (L_o) phase characterized by tight packing of lipids. In contrast, unsaturated phosphatidylcholines (PCs) are loosely packed, forming a liquid-disordered (L_d) phase surrounding the L_o phase. It is known that the L_o-L_d phase separation can be reproduced in artificial membranes consisting of three components: saturated PCs or sphingomyelins (SMs), unsaturated PCs such as 1,2-dioleoyl-*sn*-glycero-3-phosphocholine (DOPC), and cholesterol (Chol) (7–11). Therefore, the ternary mixtures are regarded as a domain structure model for understanding biophysical properties of lipid rafts. Recently, fluorescence microscopy techniques have been applied to giant unilamellar vesicles (GUVs) composed of raft-exhibiting ternary systems to observe their phase behaviors and lipid mobility (12–20), providing thermodynamic, albeit macroscopic, insights into raft model membranes.

In contrast, more atomistic information of lipid bilayers is obtainable from solid-state ^{2}H NMR spectroscopy, which provides quadrupole couplings of deuterated phospholipids and Chol, consequently yielding direct information regarding their membrane dynamics and the effect of Chol on the membranes (21–28). However, most ^{2}H NMR studies of lipid bilayers have utilized per- or multideuterated lipid molecules, which would hamper the application of ^{2}H NMR to complex membrane systems. We recently synthesized site-specifically deuterated *N*-stearoylsphingomyelin (SSM, Fig. 1 *a*) and measured their quadrupole splitting in single-component SSM and binary SSM-Chol membrane systems, which revealed accurate segmental motions of methylene groups encompassing an entire SSM molecule (29,30). In this report, we further applied the site-specifically deuterated SSMs to raft-exhibiting ternary mixtures (SSM/DOPC/Chol) and acquired the quadrupole coupling profiles of SSM from L_o and L_d domains separately and simultaneously. To our knowledge, this is the first report that shows detailed lipid chain dynamics in coexisting ordered and disordered domains. We also found that the ^{2}H NMR analysis is useful in determining the accurate mole fraction of each component distributed in L_o and L_d domains, respectively.

MATERIALS AND METHODS

Materials

DOPC was purchased from Avanti Polar Lipids (Alabaster, AL), cholesterol was purchased from Nacalai Tesque (Kyoto, Japan), and deuterium-depleted water was from ISOTEC, Inc. (Miamisburg, OH). Unlabeled SSM was purified from bovine brain SM purchased from Avanti Polar Lipids by

Submitted December 8, 2014, and accepted for publication April 6, 2015.

*Correspondence: matsmori@chem.kyushu-univ.jp

Nobuaki Matsumori's present address is Department of Chemistry, Graduate School of Sciences, Kyushu University, Higashi-ku, Fukuoka, 812-8581, Japan.

Editor: Mei Hong.

0006-3495/15/05/2502/5 $2.00

http://dx.doi.org/10.1016/j.bpj.2015.04.008

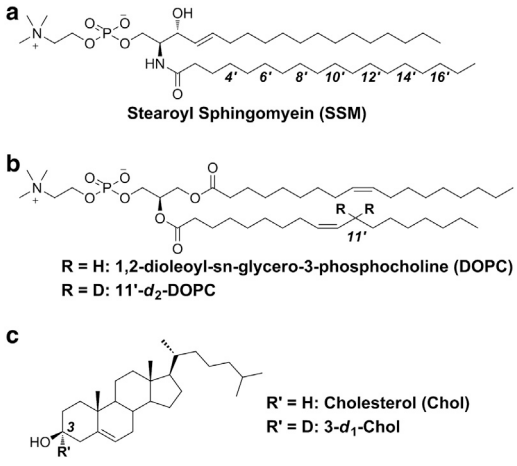

FIGURE 1 Chemical structures of compounds used in this study. (*a*) Site-specifically deuterated *N*-stearoylsphingomyelin (SSM). Each numbered position was deuterium labeled, and seven kinds of isotope isomers were used to capture the motion of SSM in membranes. (*b*) 1,2-dioleoyl-*sn*-glycero-3-phosphocholine (DOPC) and 11'-d_2-DOPC. (*c*) Cholesterol (Chol) and 3-d_1-Chol.

reverse-phase high-performance liquid chromatography as previously reported (29). Site-specific deuterium labeled SSMs (4'-, 6'-, 8'-, 10'-, 12'-, 14'-, and 16'-d_2-SSMs) (Fig. 1 *a*) and 3-d_1-Chol were synthesized as previously reported (29,31). The synthetic procedure and characterization for 11'-d_2-DOPC (Fig. 1 *b*) is described in the Supporting Material.

Sample preparation and measurements of ^{2}H NMR

Sample preparation and ^{2}H NMR measurements were conducted in a similar manner to our previous work (29). In this study, the following mixtures were prepared; 10'-d_2-SSM, DOPC, and Chol (1:1:1, 12.7 μmol each); purified SSM, DOPC, and 3-d_1-Chol (1:1:1, 14.2 μmol each); purified SSM, 11'-d_2-DOPC, and Chol (1:1:1, 9.2 μmol each); purified SSM (6.74 μmol), deuterated SSM (except 10'-d_2-SSM, 6.82 μmol), DOPC (13.6 μmol), and Chol (13.6 μmol); purified SSM (7.00 μmol), deuterated SSM (6.86 μmol), and DOPC (13.9 μmol). These mixtures were dissolved in MeOH-$CHCl_3$, and the solvent was removed in vacuo for at least 12 h. The dried membrane films were hydrated with ~1 mL of water, and vigorously vortexed at 65°C to form multilamellar vesicles. After being freeze-thawed, each suspension was lyophilized, rehydrated with deuterium-depleted water to be 50% moisture (w/w), and freeze-thawed several times. Then each sample was transferred into a 5 mm glass tube (Wilmad, Vineland, NJ), which was sealed with epoxy glue.

All the ^{2}H NMR spectra were recorded on a 300 MHz CMX300 spectrometer (Chemagnetics, Agilent, Palo Alto, CA) fitted with a 5 mm ^{2}H static probe (Otsuka Electronics, Osaka, Japan) using a quadrupolar echo sequence. The 90° pulse width was 2 μs, interpulse delay was 30 μs, and the repetition rate was 0.5 s. The sweep width was 200 MHz, and the number of scans was around 150,000.

RESULTS AND DISCUSSION

^{2}H quadrupole splitting profiles of SSM in SSM/DOPC/Chol ternary mixtures

The site-specifically deuterated SSMs were synthesized as previously reported (29). Fig. 2 shows two pairs of quadrupole splittings in the ^{2}H NMR spectrum of 10'-d_2-SSM in the ternary mixture (SSM/DOPC/Chol at a ratio of 1:1:1) at 30°C. Given that an ordered domain provides a larger quadrupole splitting, the inner and outer doublets are attributable to the deuterated SSM partitioned into the L_d and L_o phases, respectively. This spectrum clearly demonstrates that SM is not completely confined to the L_o phase but partitioned both in the L_d and L_o phases. In addition, the clear observation of two pairs of splittings suggests that the exchange of SM molecules between L_o and L_d phases does not occur or much slower than the ^{2}H NMR timescale.

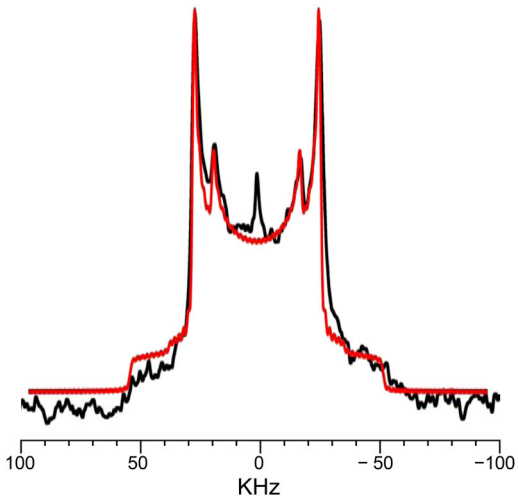

FIGURE 2 ^{2}H NMR spectrum of 10'-d_2-SSM in phase-separating ternary mixture (10'-d_2-SSM/DOPC/Chol at a ratio of 1:1:1) at 30°C. The outer and inner quadrupole doublets are attributed to the deuterated SSM distributed in the L_o and L_d domains, respectively. The red trace represents the spectral simulation to evaluate the molar ratio of SSM distributed in the L_o and L_d domains. To see this figure in color, go online.

In a similar manner, we successfully acquired quadrupole coupling data of 4'-d_2-, 6'-d_2-, 8'-d_2-, 12'-d_2-, 14'-d_2-, and 16'-d_2-SSMs distributed in the L_o and L_d domains (Table S1), which allowed us to depict the quadrupole splitting profiles of SSM at 30°C in ordered and disordered domains, respectively (Fig. 3). For comparison, the figure includes deuterium quadrupole profiles of SSM/Chol (1:1) (29) and SSM/DOPC (1:1, Table S1) binary mixtures at 30°C. However, the profile of a single-component SSM membrane is not indicated in the figure because pure SSM membranes forming a gel phase at 30°C did not give clear quadrupole couplings in the ^{2}H NMR spectra. Interestingly, the deuterium quadrupole profile from the L_o phase of the ternary system was almost identical to that of the SSM-Chol binary mixture (Fig. 3). This suggests that the order profile from the binary system is essentially applicable to more complicated membrane systems in terms of the acyl chain order. On the other hand, the deuterium quadrupole values from the L_d phase are larger than those from the SSM/DOPC mixture, suggesting that Chol is also distributed in the L_d phase to

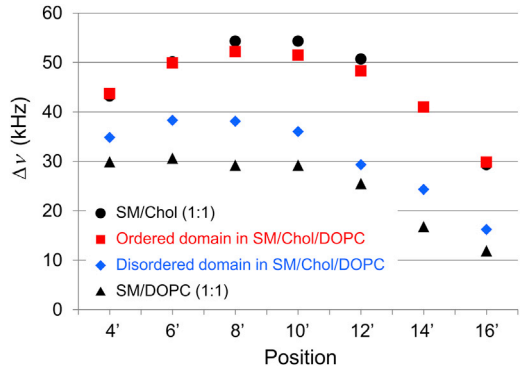

FIGURE 3 Quadrupole splitting profiles of SSM obtained from coexisting ordered and disordered domains in SM/Chol/DOPC (1:1:1) ternary mixtures at 30°C. Data from binary systems, SM/Chol (1:1) (29) and SM/DOPC (1:1), are also shown for comparison. The possible errors in the measurements were within ± 1 kHz. To see this figure in color, go online.

enhance the order of SSM as compared with the Chol-free SSM/DOPC system.

It should be emphasized that this is the first report, to our knowledge, on the order profile of lipid alkyl chains obtained from coexisting ordered and disordered phases; the lipid dynamics in phase-separated domains have never been reported even theoretically because of the infeasibility of reproducing the phase-separation of membranes by molecular dynamics simulations. In this context, this study demonstrates the use of ^{2}H NMR spectroscopy to detect the atomic-level dynamics of lipid molecules in phase-separating membranes.

Compositional mole fractions in L_o and L_d phases

As described above, the order profiles of SSM in the L_d domain demonstrated that SM is not excluded but is partitioned in the L_d domain to some extent. Moreover, these profiles suggested that Chol is distributed to the L_d phase to enhance the alkyl chain order of SSM. To understand the properties of the coexisting L_o and L_d domains precisely, it is of particular importance to assess the distribution ratio of each component in these domains. We found that the ^{2}H NMR spectra could be used to determine the distribution ratio. The mole fraction of SSM distributed to the L_o and L_d phases was evaluated to be 83:17 at 30°C (Table 1) by simulating the ^{2}H NMR spectrum, using the SIMPSON software (Fig. 2) (32). Similarly, ^{2}H NMR spectra of 3-d_1-Chol (31) and 11'-d_2-DOPC (Fig. 1, *b* and *c*), the latter of which was newly synthesized for this study, whereas 11,11'-d_4-DOPC was previously reported (33), were measured in the ternary system (Figs. 4 and S1), and their mole fractions were determined as listed in Table 1. Intriguingly, it was found that as much as 30 mol% of DOPC is partitioned in the L_o phase, and ca. 20 mol% of Chol and SSM are distributed to the L_d phase (Table 1). These data are difficult to obtain by using other methods, as discussed later, and are indispensable for understanding the mechanism of domain formation at the molecular level.

TABLE 1 Mole fraction of each component distributed in L_o and L_d phases in the SSM/Chol/DOPC (1:1:1) system

	L_o Phase[a] (%)	L_d Phase[a] (%)
SSM	83 ± 2	17 ± 2
Chol	80 ± 1	20 ± 1
DOPC	31 ± 2	69 ± 2

Data obtained at 30°C.
[a]Errors arise from manual fitting of the experimental and simulated spectra.

We also measured ^{2}H NMR spectra of the ternary mixtures at different temperatures and found that the two pairs of doublets are merged into a single pair at around 40°C (Table S2), which corresponds to the phase transition from L_o-L_d coexistence to a single liquid phase. However, according to a reported temperature-dependent phase diagram of SSM/DOPC/Chol, which was constructed using fluorescent microscopy of GUVs (20), the phase transition of the 1:1:1 mixture was supposed to occur at a lower temperature of ~35°C. This inconsistency might be attributable to the membrane perturbation and/or photo-induced lipid modification, both of which are directly related to the presence of fluorophores. In this regard, noninvasive ^{2}H NMR using minimally deuterated lipid molecules, which would induce minimal isotope effects, would be a more appropriate tool to establish sensitive phase diagrams of ternary membranes.

^{2}H NMR spectra were previously used to determine phase diagrams of binary lipid-Chol membranes (34,35) and ternary mixtures (36); however, this study is the first report, to our knowledge, that mole fractions of all of the components in membrane mixtures are estimated using ^{2}H NMR. In general, the domain composition in phase-segregated ternary mixtures can be defined by the tie-lines in a phase diagram (11); however, the procedure for determining tie-lines is rather complicated and challenging. Fig. 5 shows how our data can be used to simultaneously determine the tie-line and phase boundary in the phase diagram. Fig. S2 displays the superposition of our data with recently reported phase diagrams for the SM/DOPC/Chol system obtained from fluorescent microscopy (37), which demonstrates that, although the reported and current phase boundaries are in good agreement, the tie-line inclinations are significantly different between them. This discrepancy might indicate the difficulty and ambiguity in determining the tie-lines and the phase boundaries in phase diagrams. Hence, the merit of our ^{2}H NMR analysis is that the mole fraction of membrane lipids distributed in ordered and disordered domains is directly attainable without experimental complexity. In particular, the synthesis of deuterated compounds allows for the distribution of all components to be determined without ambiguity.

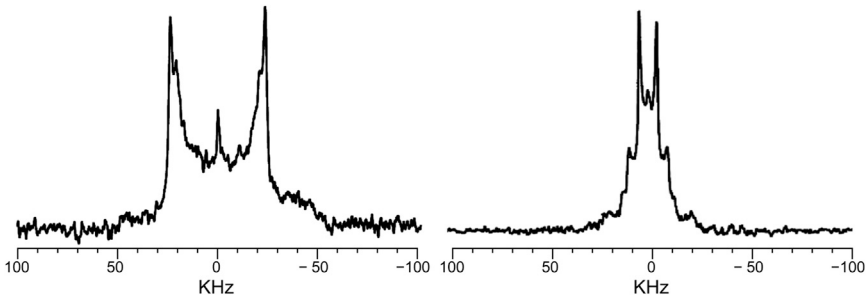

FIGURE 4 ^{2}H NMR spectra of 3-d_1-Chol (*left*) and 11'-d_2-DOPC (*right*) in phase-separating ternary mixtures (SSM/DOPC/Chol at a ratio of 1:1:1) at 30°C. The outer and inner quadrupole doublets are attributed to the deuterated components residing in the L_o and L_d phases, respectively.

Finally, we refer to the accuracy of the mole fractions obtained from ^{2}H NMR spectra. Although the manual spectral fitting causes some errors, change of 1% or 2% fraction ratio provided simulated spectra significantly different from observed ones, as reflected in Table 1. Another possible cause of error is the difference in relaxation times of ^{2}H signals from ordered and disordered domains. We therefore measured ^{2}H NMR with different interpulse delay times in the quadrupolar echo sequence and confirmed that the relaxation of ^{2}H signals gave little influence on the estimation of mole fractions up to the delay time of 100 μs.

CONCLUSIONS

In this study, for the first time to our knowledge, we successfully acquired deuterium quadrupole coupling profiles of SSM from coexisting L_o and L_d phases, separately and simultaneously. The data indicates that the quadrupole profile of the L_o phase in an SSM/DOPC/Chol ternary system shows close similarity to that in an SSM-Chol binary mixture, although a significant amount of DOPC is partitioned to the L_o phase. This observation suggests that, in the presence of Chol, SSM is not molecularly miscible with DOPC and possibly forms small (nanometer-scale) clusters.

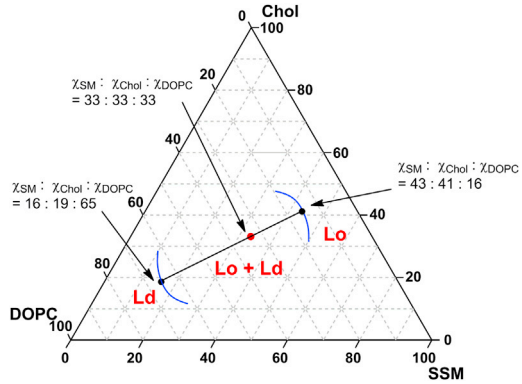

FIGURE 5 Tie-line and phase boundary in the phase diagram for SSM/DOPC/Chol. The red point marks 1:1:1 composition, and the black points are obtained from Table 1, which represent phase boundaries between ($L_o + L_d$) and L_o phases and between ($L_o + L_d$) and L_d phases, as hypothetically shown by the blue curves. These three points lie on a straight line, which is the tie-line. To see this figure in color, go online.

We also demonstrated that ^{2}H NMR spectroscopy, in combination with organic synthesis of deuterated components, could be used to reveal the accurate mole fractions of each component distributed in the L_o and L_d phases. Relative lipid composition of the L_d/L_o domains provides rich thermodynamic information, particularly on drawing and/or verifying phase diagrams. Mole composition data are further utilized not only for examining the effect of membrane-acting peptides and organic compounds, some of which are known to modulate raft domains (38), on compositional distributions of membranes, but also for extracting molecular interactions by computer simulations. In fact, molecular dynamics simulations of ternary mixtures are currently underway using the compositional distribution obtained in this study. These simulations, in combination with lipid order profiles separately obtained from coexisting domains, will further provide a deeper understanding of the phase separation and consequently the molecular mechanism of lipid raft formation.

SUPPORTING MATERIAL

Supporting Methods, two figures, and two tables are available at http://www.biophysj.org/biophysj/supplemental/S0006-3495(15)00386-0.

AUTHOR CONTRIBUTIONS

N.M. and M.M. designed research, T.Y. and N.M. performed research, H.T. contributed organic synthesis, and all authors analyzed data. N.M. and M.M. wrote the article.

ACKNOWLEDGMENTS

The authors thank Drs. Yuichi Umegawa and Naoya Inazumi, Osaka University, in our department for help in ^{2}H NMR measurements. This work was supported by Grants-in-Aid for Scientific Research (A) (No. 25242073) from MEXT, Japan; a grant from the Suntory Institute for Bioorganic Research, Japan; and the ERATO "Lipid Active Structure Project" from the Japan Science and Technology Agency (JST). T.Y. as a JSPS fellow is grateful to the Japan Society for the Promotion of Science.

REFERENCES

1. Simons, K., and E. Ikonen. 1997. Functional rafts in cell membranes. *Nature.* 387:569–572.

2. Anderson, R. G. W., and K. Jacobson. 2002. A role for lipid shells in targeting proteins to caveolae, rafts, and other lipid domains. *Science.* 296:1821–1825.
3. Binder, W. H., V. Barragan, and F. M. Menger. 2003. Domains and rafts in lipid membranes. *Angew. Chem. Int. Ed. Engl.* 42:5802–5827.
4. Simons, K., and D. Toomre. 2000. Lipid rafts and signal transduction. *Nat. Rev. Mol. Cell Biol.* 1:31–39.
5. Ikonen, E. 2001. Roles of lipid rafts in membrane transport. *Curr. Opin. Cell Biol.* 13:470–477.
6. Brown, D. A., and E. London. 1998. Functions of lipid rafts in biological membranes. *Annu. Rev. Cell Dev. Biol.* 14:111–136.
7. Silvius, J. R. 1992. Cholesterol modulation of lipid intermixing in phospholipid and glycosphingolipid mixtures. Evaluation using fluorescent lipid probes and brominated lipid quenchers. *Biochemistry.* 31:3398–3408.
8. Silvius, J. R., D. del Giudice, and M. Lafleur. 1996. Cholesterol at different bilayer concentrations can promote or antagonize lateral segregation of phospholipids of differing acyl chain length. *Biochemistry.* 35:15198–15208.
9. Ahmed, S. N., D. A. Brown, and E. London. 1997. On the origin of sphingolipid/cholesterol-rich detergent-insoluble cell membranes: physiological concentrations of cholesterol and sphingolipid induce formation of a detergent-insoluble, liquid-ordered lipid phase in model membranes. *Biochemistry.* 36:10944–10953.
10. Xu, X., and E. London. 2000. The effect of sterol structure on membrane lipid domains reveals how cholesterol can induce lipid domain formation. *Biochemistry.* 39:843–849.
11. de Almeida, R. F. M., A. Fedorov, and M. Prieto. 2003. Sphingomyelin/phosphatidylcholine/cholesterol phase diagram: boundaries and composition of lipid rafts. *Biophys. J.* 85:2406–2416.
12. Dietrich, C., L. A. Bagatolli, …, E. Gratton. 2001. Lipid rafts reconstituted in model membranes. *Biophys. J.* 80:1417–1428.
13. Baumgart, T., S. T. Hess, and W. W. Webb. 2003. Imaging coexisting fluid domains in biomembrane models coupling curvature and line tension. *Nature.* 425:821–824.
14. Kahya, N., D. Scherfeld, …, P. Schwille. 2003. Probing lipid mobility of raft-exhibiting model membranes by fluorescence correlation spectroscopy. *J. Biol. Chem.* 278:28109–28115.
15. Veatch, S. L., and S. L. Keller. 2002. Organization in lipid membranes containing cholesterol. *Phys. Rev. Lett.* 89:268101.
16. Veatch, S. L., and S. L. Keller. 2003. A closer look at the canonical 'raft mixture' in model membrane studies. *Biophys. J.* 84:725–726.
17. Veatch, S. L., and S. L. Keller. 2003. Separation of liquid phases in giant vesicles of ternary mixtures of phospholipids and cholesterol. *Biophys. J.* 85:3074–3083.
18. Veatch, S. L., and S. L. Keller. 2005. Miscibility phase diagrams of giant vesicles containing sphingomyelin. *Phys. Rev. Lett.* 94:148101.
19. Smith, A. K., and J. H. Freed. 2009. Determination of tie-line fields for coexisting lipid phases: an ESR study. *J. Phys. Chem. B.* 113:3957–3971.
20. Farkas, E. R., and W. W. Webb. 2010. Precise and millidegree stable temperature control for fluorescence imaging: application to phase transitions in lipid membranes. *Rev. Sci. Instrum.* 81:093704.
21. Seelig, J. 1977. Deuterium magnetic resonance: theory and application to lipid membranes. *Q. Rev. Biophys.* 10:353–418.
22. Leftin, A., and M. F. Brown. 2011. An NMR database for simulations of membrane dynamics. *Biochim. Biophys. Acta.* 1808:818–839.
23. Mehnert, T., K. Jacob, …, K. Beyer. 2006. Structure and lipid interaction of N-palmitoylsphingomyelin in bilayer membranes as revealed by ^{2}H-NMR spectroscopy. *Biophys. J.* 90:939–946.
24. Bunge, A., P. Müller, …, D. Huster. 2008. Characterization of the ternary mixture of sphingomyelin, POPC, and cholesterol: support for an inhomogeneous lipid distribution at high temperatures. *Biophys. J.* 94:2680–2690.
25. Bartels, T., R. S. Lankalapalli, …, M. F. Brown. 2008. Raftlike mixtures of sphingomyelin and cholesterol investigated by solid-state ^{2}H NMR spectroscopy. *J. Am. Chem. Soc.* 130:14521–14532.
26. Leftin, A., T. R. Molugu, …, M. F. Brown. 2014. Area per lipid and cholesterol interactions in membranes from separated local-field (^{13})C NMR spectroscopy. *Biophys. J.* 107:2274–2286.
27. Martinez, G. V., E. M. Dykstra, …, M. F. Brown. 2002. NMR elastometry of fluid membranes in the mesoscopic regime. *Phys. Rev. E Stat. Nonlin. Soft Matter Phys.* 66:050902.
28. Martinez, G. V., E. M. Dykstra, …, M. F. Brown. 2004. Lanosterol and cholesterol-induced variations in bilayer elasticity probed by ^{2}H NMR relaxation. *Langmuir.* 20:1043–1046.
29. Matsumori, N., T. Yasuda, …, M. Murata. 2012. Comprehensive molecular motion capture for sphingomyelin by site-specific deuterium labeling. *Biochemistry.* 51:8363–8370.
30. Yasuda, T., M. Kinoshita, …, N. Matsumori. 2014. Detailed comparison of deuterium quadrupole profiles between sphingomyelin and phosphatidylcholine bilayers. *Biophys. J.* 106:631–638.
31. Matsumori, N., Y. Kasai, …, K. Nomura. 2008. Orientation of fluorinated cholesterol in lipid bilayers analyzed by 19F tensor calculation and solid-state NMR. *J. Am. Chem. Soc.* 130:4757–4766.
32. Bak, M., J. T. Rasmussen, and N. C. Nielsen. 2000. SIMPSON: a general simulation program for solid-state NMR spectroscopy. *J. Magn. Reson.* 147:296–330.
33. van Duyl, B. Y., D. Ganchev, …, J. A. Killian. 2003. Sphingomyelin is much more effective than saturated phosphatidylcholine in excluding unsaturated phosphatidylcholine from domains formed with cholesterol. *FEBS Lett.* 547:101–106.
34. Thewalt, J. L., and M. Bloom. 1992. Phosphatidylcholine: cholesterol phase diagrams. *Biophys. J.* 63:1176–1181.
35. Vist, M. R., and J. H. Davis. 1990. Phase equilibria of cholesterol/dipalmitoylphosphatidylcholine mixtures: ^{2}H nuclear magnetic resonance and differential scanning calorimetry. *Biochemistry.* 29:451–464.
36. Veatch, S. L., I. V. Polozov, …, S. L. Keller. 2004. Liquid domains in vesicles investigated by NMR and fluorescence microscopy. *Biophys. J.* 86:2910–2922.
37. Bezlyepkina, N., R. S. Gracià, …, R. Dimova. 2013. Phase diagram and tie-line determination for the ternary mixture DOPC/eSM/cholesterol. *Biophys. J.* 104:1456–1464.
38. Tsukamoto, M., K. Kuroda, …, K. Yasuhara. 2014. Modulation of raft domains in a lipid bilayer by boundary-active curcumin. *Chem. Commun. (Camb.).* 50:3427–3430.

Supporting Materials

Deuterium NMR of Raft Model Membranes Reveals Domain-Specific Order Profiles and Compositional Distribution

Tomokazu Yasuda,[†‡] Hiroshi Tsuchikawa,[†] Michio Murata,[†‡] and Nobuaki Matsumori[†*]

[†]Department of Chemistry, Graduate School of Science, Osaka University, Toyonaka, Osaka 560-0043, Japan; [‡]Japan Science and Technology Agency, ERATO, Lipid Active Structure Project, Toyonaka, Osaka 560-0043, Japan:

Nobuaki Matsumori's present address is Department of Chemistry, Graduate School of Sciences, Kyushu University, Higashi-ku, Fukuoka, 812-8581, Japan.

Supplementary Method

General information for synthesis:

1-oleoyl-2-hydroxy-sn-glycero-3-phosphocholine was purchased from Avanti Polar Lipids. Other chemicals and solvents were purchased from Nacalai Tesque, Aldrich, TCI, and KANTO Chemicals Inc., and used without further purification unless otherwise noted. Merck precoated silica gel 60 F-254 plates and silica gel 60 (100-200 um) were used for thin layer chromatography and column chromatography, respectively. Proton nuclear magnetic resonance spectra were collected on a JEOL ECS 400 (400 MHz). Mass spectrometry was performed on a LTQ-Orbitrap XL (Thermo Scientific). Voltex mixers of VOLTEX-2GENIE (Scientific Industries) and ultrasonic cleaner BRANSON 1510 (Yamato Inc.) were used for liposome preparation.

Synthesis of 11'-d_2 -DOPC

11,11-d_2-oleic acid was synthesized as previously reported (1,2). To a solution of 1-oleoyl-2-hydroxy-*sn*-glycero-3-phosphocholine (95.1 mg, 0.18 mmol) and 11,11-d_2-oleic acid (61.4 mg, 0.22 mmol) in CH_2Cl_2 (5.0 mL) were added 2-methyl-6-nitrobenzoic anhydride (310 mg, 0.90 mmol) and *N*,*N*-dimethyl-4-aminopyridine (220 mg, 1.80 mmol).

After the reaction mixture was stirred for 14 h at room temperature, the reaction was quenched with MeOH, and solvent was evaporated to give a crude product. Purification by silica gel column chromatography ($CHCl_3$/MeOH = 3/1 to $CHCl_3$/MeOH/H_2O = 65/25/4) afforded 11'-d_2-DOPC (114 mg. 145 μmol, 81%) as a white solid. R_f 0.52 (silica gel, $CHCl_3$/MeOH/H_2O = 65/25/4); ^{1}H NMR (400 MHz, CD_3OD) δ 5.38-5.27 (4H, m, H9', H10'), 5.25 (1H, br, H2), 4.41 (1H, dd, *J* = 12.4, 3.2 Hz, H1), 4.24 (2H, br, α), 4.15 (1H, dd, *J* = 12.0, 6.8 Hz, H1), 3.98 (2H, t, *J* = 6.3 Hz, H3), 3.62 (2H, t, *J* = 4.8 Hz, β), 3.20 (9H, s, -N^+Me_3), 2.30 (4H, m, H2'), 2.03 (6H, br, H8', H11), 1.60 (4H, br, H3'), 1.25 (40 H, s, -CH_2-), 0.89 (6H, t, *J* = 6.4 Hz, H18'); ESI-HRMS m/z calcd for $C_{44}H_{82}D_2NO_8PNa^+$ $(M+Na)^+$ 810.5952, found 810.5959.

Supplementary Figures

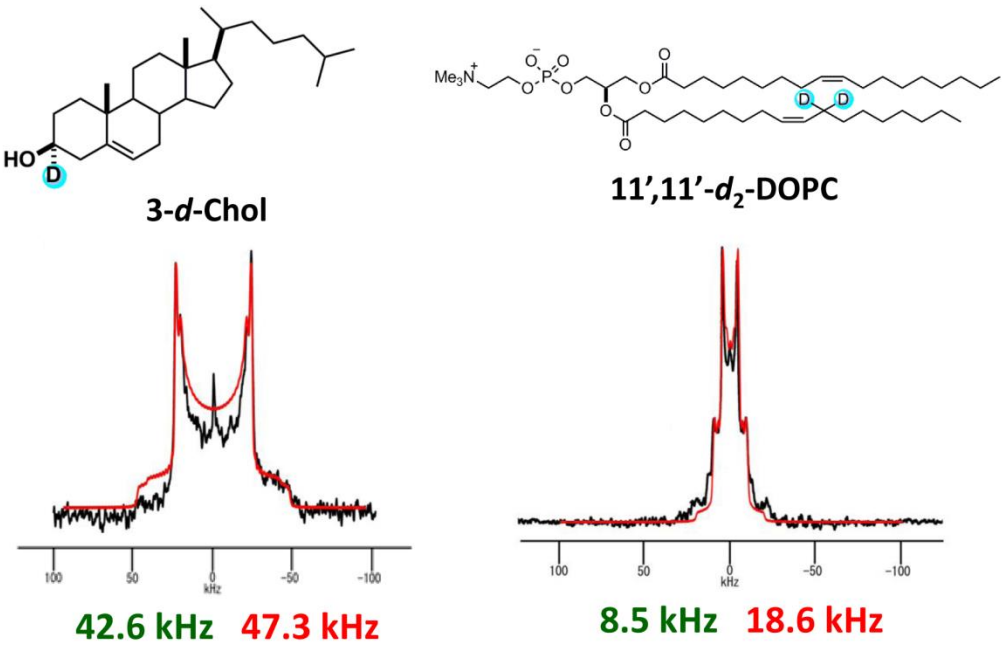

FIGURE S1 ^{2}H NMR spectra of 3-*d*-Chol and 11'-d_2-DOPC in phase-separating ternary mixture (SSM/DOPC/Chol at a ratio of 1:1:1) at 30 °C. The red traces represent the spectral simulation to evaluate the molar ratios of Chol and DOPC distributed in the L_o and L_d domains.

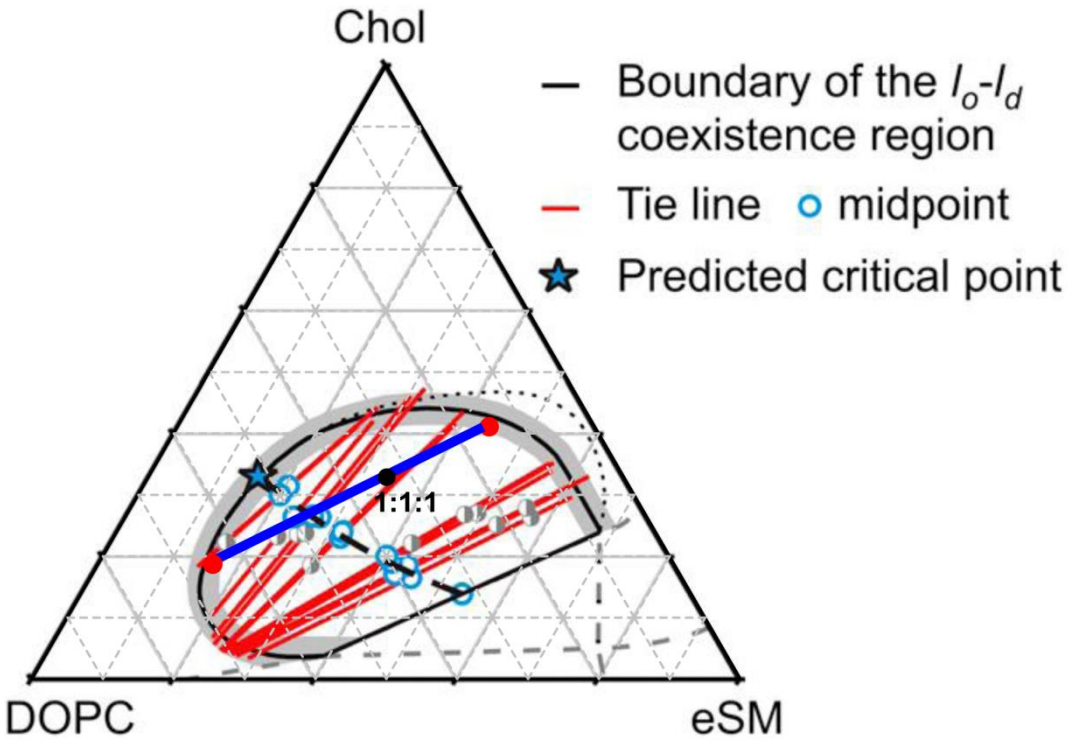

FIGURE S2 Superposition of the currently-obtained tie line (blue line) and the reported phase diagram of the DOPC/SM/Chol mixture at 23 °C. The phase diagram is from ref [3]. The solid black curve indicates the boundary of the L_o-L_d phase with ±2 mol % deviation in gray. The red points indicate the currently estimated phase boundary, and blue line is tie line containing the 1:1:1 composition.

Supplementary Tables

Table S1. Quadrupolar couplings (kHz) of deuterated SSM in membranes at 30 °C

	SSM/DOPC (1:1)	SSM/DOPC/Chol (1:1:1)
4'-d_2-SSM	29.9	34.8, 43.7
6'-d_2-SSM	30.6	38.3, 49.9
8'-d_2-SSM	29.2	38.1, 52.2
10'-d_2-SSM	29.2	36.0, 51.5
12'-d_2-SSM	25.5	29.3, 48.3
14'-d_2-SSM	16.8	24.3, 41.0
16'-d_2-SSM	11.9	16.2, 29.8

Table S2. Quadrupolar couplings (kHz) of each component in ternary membranes

	10'-d_2-SSM	11'-d_2-DOPC	3-d_1-Chol
20 °C	34.3, 53.5	8.6, 20.0	-[a]
30 °C	36.0, 51.5	8.5, 18.6	42.6, 47.0
40 °C	38.4, 49.6	9.7, 15.9	44.5
45 °C	43.3	11.4	44.4
50 °C	-[a]	-[a]	43.0

[a] Not determined.

Supporting References

[1] V. Chupin, J. A. Killian, and B. de Kruijff. 1987. ^{2}H-nuclear magnetic resonance investigations on phospholipid acyl chain order and dynamics in the gramicidin-induced hexagonal H_{II} phase. *Biophys. J.* 51:395–405.

[2] H. Chen, and E. Plettner. 2012. Site-specific ^{2}H labelled oleic acid and derived esters for use as tracers of ethyl oleate methabolism in honey bees. *Label. Compd. Radiopharm.* 55:66–70.

[3] Bezlyepkina, N., R. S. Gracià, P. Shchelokovskyy, R. Lipowsky, and R. Dimova. 2013. Phase diagram and tie-line determination for the ternary mixture DOPC/eSM/Cholesterol. *Biophys. J.* 104:1456–1464.